Crystal structure and Kondo lattice behavior of $CeNi_9Si_4$

H. Michor,* St. Berger, M. El-Hagary, C. Paul, E. Bauer, and G. Hilscher
Institut für Festkörperphysik, Technische Universität Wien, Wiedner Hauptstrasse 8–10, A-1040 Wien, Austria

P. Rogl
Institut für Physikalische Chemie, Universität Wien, Währingerstrasse 42, A-1090 Wien, Austria

G. Giester
Institut für Mineralogie und Kristallographie, Universität Wien, Althanstrasse 14, A-1090 Wien, Austria
(Received 20 January 2003; published 20 June 2003)

We have studied the crystal chemistry and magnetic, thermodynamic, and transport properties of RNi_9Si_4 with R=La and Ce. These compounds crystallize in a fully ordered tetragonal (space group $I4/mcm$) variant of the cubic $NaZn_{13}$ type. The low-temperature properties characterize $CeNi_9Si_4$ as a Kondo lattice with a large Sommerfeld value $\gamma = 155(5)$ mJ/mol K^2 as compared to $\gamma = 33$ mJ/mol K^2 of Pauli paramagnetic $LaNi_9Si_4$. The temperature dependencies of the specific heat and susceptibility are well described by the degenerate ($J = 5/2$) Coqblin-Schrieffer model with a characteristic temperature $T_0 \simeq 180$ K. The large Ce-Ce spacing in $CeNi_9Si_4$ ($d_{\text{Ce-Ce}} \approx 5.6$ Å) implies very weak Ce-Ce intersite exchange interactions which is corroborated by the thermoelectric power $S(T)$ showing close agreement with theoretical results of the degenerate Anderson lattice without intersite interactions. $CeNi_9Si_4$ appears to be a model type Kondo lattice system with $T_0 > \Delta_{\text{CEF}} \gg T_{\text{RKKY}}$ where T_0, Δ_{CEF} (crystalline electric field), and T_{RKKY} (Ruderman-Kittel-Kasuya-Yosida) are the characteristic energy scales of the Kondo interaction, crystal field splitting, and Ce-Ce intersite exchange coupling, respectively. $CeNi_9Si_4$ shows a remarkably low ratio $A/\gamma^2 = 0.83\ (8) \times 10^{-6}\ \mu\Omega$ cm(molK/mJ)^2 which is one order-of-magnitude smaller than the usual Kadowaki-Woods ratio of heavy-fermion systems.

DOI: 10.1103/PhysRevB.67.224428 PACS number(s): 61.66.−f, 65.40.−b, 71.27.+a, 72.15.−v

I. INTRODUCTION

Cerium-based intermetallic compounds exhibit a rich variety of ground-state properties due to the competition between three different types of interactions: crystal-field effects, Ce-Ce intersite correlations provoking the formation of long-range magnetic order, and on-site correlations between $4f$- and conduction-electron states prompting the formation of a local Kondo singlet. In the case of stronger hybridization, cerium shows an intermediate valence. There is a significant number of compounds with $k_B T_{\text{RKKY}}$ (Ruderman-Kittel-Kasuya-Yosida) $\sim k_B T_K$, i.e., antiferromagnetic heavy-fermion systems[1] and compounds showing quantum critical phenomena, e.g., $Ce(Cu,Au)_6$, $CeCu_2Si_2$, and $CeNi_2Ge_2$ (Refs. 2 and 3) ($k_B T_{\text{RKKY}}$ is the binding energy of the Néel state and $k_B T_K$ the Kondo energy). On the other hand, it is difficult to find simple integer valent ($n_{4f} \simeq 1$) Kondo lattices with large enough Ce-sublattice spacing such that intersite correlations are negligible. An interesting candidate in this respect is the partially disordered tetragonal compound $CeNi_{8.5}Si_{4.5}$ which is a ternary member of the Ce-Ni-Si phases.[4] A neutron-diffraction study by Moze *et al.*[5] essentially confirmed the symmetry and atom parameters published by Bodak[4] and revealed a strong site preference of Si to one particular lattice position (see Sec. III A for details). Nevertheless, the exact stoichiometry and width of formation of this Ce-Ni-Si phase remained unclear because Moze *et al.*[5] noted the presence of impurity phases in their sample with nominal composition $Ce_2Ni_{17}Si_9$.

In this paper we present a reinvestigation of the homogeneity region and crystal structure of the previously reported $CeNi_{8.5}Si_{4.5}$ phase and demonstrate the existence of fully ordered stoichiometric $CeNi_9Si_4$ and $LaNi_9Si_4$ compounds as a distortion variant of the cubic $NaZn_{13}$ type. $LaNi_9Si_4$ has been studied as an isostructural nonmagnetic reference for $CeNi_9Si_4$. The investigation of magnetic, thermodynamic, and transport properties of the latter reveals a nonmagnetic Kondo lattice with an extraordinary position among Kondo lattices because of the very low fraction of cerium in this compound (7 at.%) and accordingly the large Ce-Ce distance $d_{\text{Ce-Ce}} \approx 5.6$ Å (see, for comparison, the overview on Ce compounds compiled by Sereni[1]) which suggests that the Ce-Ce intersite interactions are very weak. A similar position among Yb-Kondo-lattice systems has been considered for $YbCu_4Ag$ initially reported by Rossel *et al.*[6] Some interesting analogies between $CeNi_9Si_4$ and $YbCu_4Ag$ are discussed, e.g., in context with the exceptional behavior of the thermoelectric power and with the ratio $A/\gamma^2 \sim 10^{-6}\ \mu\Omega$ cm(mol K/mJ)^2 one order-of-magnitude smaller as compared to the typical Kadowaki-Woods[7] ratio $A/\gamma^2 \sim 10^{-5}\ \mu\Omega$ cm(molK/mJ)^2 observed for the majority of heavy-fermion systems.

II. EXPERIMENTAL DETAILS

Polycrystalline samples $LaNi_9Si_4$ and $CeNi_{9-x}Si_{4+x}$ with $x = 0.0$, 0.2, and 0.4 were synthesized by high-frequency induction melting on a water cooled copper hearth under a protective argon atmosphere. The starting materials were Ce and La ingots (Johnson-Matthey, Great Britian, 99.95% vacuum remelted) and Ni and Si ingots (both Johnson-Matthey, 99.999%). In a first step, Ni and Si were melted

together to produce a master alloy, which was then melted together with the Ce ingot. To ensure homogeneity the alloy buttons were broken and remelted several times. For the final annealing treatment samples were wrapped in Ta foil, sealed in an evacuated quartz capsule, and heated for one week at 990°C.

In order to reexamine the formation of $CeNi_{8.5}Si_{4.5}$ and the corresponding homogeneity region we carefully checked the phase purity of the series $CeNi_{9-x}Si_{4+x}$ with $x=0.0$, 0.2 and 0.4 by x-ray powder diffraction (Guinier, with an image plate recording system; Cu$K_{\alpha 1}$ radiation) and electron microprobe analyses (EMPA) based on energy dispersive x-ray spectroscopy. Quantitative Rietveld refinements were performed employing the program package FULLPROF.[8] Small single crystals of $LaNi_9Si_4$ and $CeNi_9Si_4$ were selected for structure investigation at room temperature on a four circle Nonius Kappa diffractometer equipped with a charge coupled device (CCD) area detector (graphite monochromatic MoK_α radiation, $\lambda=0.071073$ nm). Orientation matrix and unit-cell parameters were derived using the program DENZO.[9] Due to the small crystal size, the rather uniform crystal shape, and particularly the small linear absorption coefficient for Mo radiation no absorption correction was made. The crystal structure was refined with the aid of the SHELXS-97 program.[10]

Low- (2–300 K) and high-temperature (294–550 K) electrical resistivity measurements were performed in a He-bath cryostat and in an evacuated furnace, respectively, both on bar-shaped samples, applying a standard four-probe dc method with gold pins as voltage and current contacts in the former case and W26%Re pins in the latter case. Thermopower measurements at low (5–300 K) and high temperature (315–850 K) were performed with a differential method. The absolute thermopower $S_x(T)$ was calculated using the following equation: $S_x(T)=S_{Ref}(T)-V_{Ref,x}/\Delta T$ where S_{Ref} is the absolute thermopower of lead in the low-temperature case and the absolute thermopower of platinum in the high temperature case. $V_{Ref,x}$ is the thermally induced voltage across the sample, depending on the temperature difference ΔT. dc susceptibility measurements were performed in a 6-T superconducting quantum interference device magnetometer. Specific-heat measurements were carried out on samples of about 1 g in the temperature range 1.5 K–140 K, employing a quasi adiabatic step heating technique.

III. EXPERIMENTAL RESULTS

A. Compound formation and structural chemistry

Rietveld refinements of the x-ray patterns of $CeNi_{9-x}Si_{4+x}$ with $x=0.0$, 0.2, and 0.4 revealed a single phase pattern only for the stoichiometric sample $CeNi_9Si_4$, while additional reflections were observed for $x=0.2$ and 0.4. These findings are corroborated by EMPA revealing the presence of traces of binary Ni-Si phases for stoichiometric $CeNi_9Si_4$ and an increasing amount of binary phases for off-stoichiometric samples with $x=0.2$ and in particular, for $x=0.4$. While the nominal composition of the main phase $CeNi_9Si_4$ and $CeNi_{8.8}Si_{4.2}$ is confirmed within the resolution of the experiment (about 0.5 at.%), the EMPA data indicate an approximate formula $CeNi_{8.8}Si_{4.2}$ for the sample with the nominal composition $CeNi_{8.6}Si_{4.4}$ suggesting a small homogeneity region extending towards slightly higher Si contents.

Analysis of the four circle x-ray single-crystal data confirmed for both crystals, $LaNi_9Si_4$ and $CeNi_9Si_4$, tetragonal symmetry with $I4/mcm$ as the highest symmetrical space group. Employing those atom parameters as previously assigned to $CeNi_{8.5}Si_{4.5}$ by Bodak[4] revealed convincingly low residual values which confirmed the general atom arrangement. Atomic thermal displacement parameters, however, require a fully ordered arrangement with Ni atoms at the 4*d* sites and Si atoms only located at the 16l sites, in agreement with the stoichiometric composition RNi_9Si_4. This result unambiguously holds for both $LaNi_9Si_4$ and $CeNi_9Si_4$. Occupancies of all crystallographic sites were refined but did not reveal any significant deviations from stoichiometry. Refining anisotropic thermal displacement factors in the final run yielded *R* values as low as 0.015, confirming the structural model with full atom order for both crystal specimens investigated. Results of the structure determination are summarized in Table I.

The strong preference of Ni atoms for the 4*d* site was noted earlier by Moze *et al.*[5] from a neutron-diffraction study of $Ce_2Ni_{17}Si_9$ placing Si atoms in excess of the stoichiometric composition into the 16*k* position, thus, making this position randomly occupied by Si and Ni atoms. This observation is in perfect agreement with our Rietveld refinement for the sample with nominal composition $CeNi_{8.6}Si_{4.4}$, where Ni atoms are undoubtedly located at the 4*d* sites and Si atoms are found to share the 16*k* positions with Ni. The tetragonal crystal structure of $CeNi_9Si_4$ is thus a fully ordered distorted variant of the cubic $NaZn_{13}$ parent type. A corresponding atom distribution was also derived by Tang *et al.*[12] from a powder diffraction study of $LaFe_9Si_4$. Close structural relations exist to the structures of $CaCu(Al,Cu)_{12}$ (partly ordered $NaZn_{13}$-type) and to the $Pr_{1-\delta}Co_9Ge_4$-type,[13] which is an occupation variant with respect to $CeNi_9Si_4$ and in addition exhibits defects at the rare earth site.

Information on the phase relations within the systems La-Ni-Si and Ce-Ni-Si has been summarized by Rogl,[14] but has to be modified in light of the data obtained in this study: the single phase regions attributed to the tetragonal $CeNi_9Si_4$-type phases, originally given at 800°C as $LaNi_{8.8-8.4}Si_{4.2-4.6}$ and $CeNi_{8.6-8.4}Si_{4.4-4.6}$, will have to be slightly shifted to accommodate the stoichiometric composition RNi_9Si_4, at least at higher temperatures.

B. Magnetic and specific-heat measurements

Isothermal magnetization measurements, $M(H)$, up to 6 T reveal for $LaNi_9Si_4$ and $CeNi_9Si_4$ essentially linear paramagnetic behavior (see the 2-K data in Fig. 1) which is in good agreement with the dc magnetic susceptibilities $\chi(T)$ measured from 2–300 K in static magnetic fields of 0.1 T, 1 T, and 3 T. The temperature dependence of these susceptibilities is shown in Fig. 2. $LaNi_9Si_4$ shows an essentially temperature-independent magnetic susceptibility revealing Pauli paramagnetism with $\chi_0 \simeq 0.6\times 10^{-3}$ emu/mol. $CeNi_9Si_4$ on the other hand exhibits a typical Kondo-like behavior of $\chi(T)$ with a nearly constant low-temperature

TABLE I. X-ray single-crystal data for $LaNi_9Si_4$ and $CeNi_9Si_4$; ordered variant of the $NaZn_{13}$ type, space group $I4/mcm$; No. 140. Data were collected on a Nonius Kappa CCD; MoK_α; redundancy >8. Crystal structure data were standardized using the program TYPIX (Ref. 11) RE represents rare-earth metals.

Parameter/compound	$LaNi_9Si_4$	$CeNi_9Si_4$
Crystal size	$56\times84\times84$ μm^3	$56\times72\times56$ μm^3
a; c (nm)	$a=0.78723(1)$; $c=1.14807(2)$	$a=0.7846(1)$; $c=1.1453(2)$
ρ_x (Mgm^{-3}); μ_{abs} (mm^{-1})	7.279; 29.67	7.357; 30.34
Data collection, 2Θ range (°)	$2\leqslant2\Theta\leqslant72.6$	$2\leqslant2\Theta\leqslant72.4$
Frames	90 sec/frame; 399 frames; nine sets	115 sec/frame; 385 frames, eight sets
Reflections in refinement	$475\geqslant4\sigma(F_o)$ of 488	$464\geqslant4\sigma(F_o)$ of 483
Mosaicity	<0.8	<1.1
Number of variables	25	25
$R_{F^2}=\Sigma\lvert F^2_{obs}-F^2_{calc}\rvert/\Sigma\lvert F^2_{obs}\rvert$	0.0129	0.0146
R_{Int}	0.044	0.044
$wR2$	0.030	0.031
GOF	1.133	1.173
Extinction (Zachariasen)	0.0014(1)	0.0012(1)
RE in $4a$ $(0,0,\frac{1}{4})$; occupancy	1.0	1.0
$U_{11}=U_{22}$; U_{33}; $U_{12}=U_{13}=U_{23}=0.0$	0.00498(7); 0.0063(1)	0.00518(8); 0.0078(1)
Ni1 in $16k$ $(x,y,0)$;	$x=0.06865(3)$; $y=0.20405(3)$	$x=0.06876(4)$; $y=0.20352(4)$
Occupancy;	1.0	1.0
U_{11}; U_{22}; U_{33}	0.0059(1); 0.0053(1); 0.0069(1)	0.0056(1); 0.0051(1); 0.0080(1)
U_{12}; $U_{13}=U_{23}=0.0$	0.00026(8)	0.00022(8)
Ni2 in $16l$ $(x,x+\frac{1}{2},z)$	$x=0.62953(2)$; $z=0.18429(2)$	$x=0.63007(3)$; $z=0.18443(3)$
Occupancy	1.0	1.0
$U_{11}=U_{22}$; U_{33}	0.00733(9); 0.0048(1)	0.00720(9); 0.0057(1)
U_{12}; $U_{13}=U_{23}$	0.00040(8); 0.00072(6)	0.00025(9); 0.00078(6)
Ni3 in $4d$ $(0,\frac{1}{2},0)$; occupancy	1.0	1.0
$U_{11}=U_{22}$; U_{33}	0.0052(1); 0.0068(2)	0.0052(1); 0.0068(2)
U_{12}; $U_{13}=U_{23}=0.0$	0.0006(2)	0.0007(2)
Si in $16l$ $(x,x+\frac{1}{2},z)$;	$x=0.17071(5)$; $z=0.11786(5)$	$x=0.17066(6)$; $z=0.11819(6)$
Occupancy;	1.0	1.0
$U_{11}=U_{22}$; U_{33}	0.0066(1); 0.0055(2)	0.0066(2); 0.0063(2)
U_{12}; $U_{13}=U_{23}$	$-0.0012(2)$; $-0.00009(10)$	$-0.0012(2)$; 0.00005(13)
Residual density; max; min [electrons/nm^3]$\times1000$	0.86; -0.98	0.95; -0.71
Principal mean-square atomic displacements $U_{ij}\times100$ nm^2	La 0.0063 0.0050 0.0050 Ni1 0.0069 0.0060 0.0052 Ni2 0.0080 0.0069 0.0045 Ni3 0.0068 0.0058 0.0046 Si 0.0078 0.0056 0.0053	Ce 0.0078 0.0052 0.0052 Ni1 0.0080 0.0057 0.0051 Ni2 0.0080 0.0070 0.0051 Ni3 0.0075 0.0059 0.0044 Si 0.0078 0.0063 0.0053
	Interatomic distances (nm); standard deviations generally <0.0005 nm	
CN=24	La 8 Ni2 0.31803 8 Si 0.32905 8 Ni1 0.33332	Ce 8 Ni2 0.31670 8 Si 0.32786 8 Ni1 0.33225
CN=10(12)	Ni1 1 Ni3 0.23917 2 Ni1 0.23968 2 Si 0.24718 2 Si 0.25206 1 Ni1 0.25305 2 Ni2 0.25343 (2 La 0.33332)	Ni1 2 Ni1 0.23836 1 Ni3 0.23879 2 Si 0.24655 m2 Si 0.25171 1 Ni1 0.25268 2 Ni2 0.25294 (2 Ce 0.33225)

TABLE I. (*Continued.*)

Parameter/compound	$LaNi_9Si_4$	$CeNi_9Si_4$
CN=9(11)	Ni2 1 Si 0.23173 Ni2	1 Si 0.23050
	1 Si 0.23511	1 Si 0.23376
	2 Si 0.25046	2 Si 0.24989
	2 Ni1 0.25343	2 Ni1 0.25294
	2 Ni2 0.25369	2 Ni2 0.25341
	1 Ni3 0.25605	1 Ni3 0.25583
	(2 La 0.31803)	(2 Ce 0.31670)
CN=12	Ni3 4 Si 0.23330	Ni3 4 Si 0.23277
	4 Ni1 0.23917	4 Ni1 0.23879
	4 Ni2 0.25605	4 Ni2 0.25583
CN=10(12)	Si 1 Ni2 0.23173	Si 1 Ni2 0.23050
	1 Ni3 0.23330	1 Ni3 0.23277
	1 Ni2 0.23511	1 Ni2 0.23376
	2 Ni1 0.24718	2 Ni1 0.24655
	2 Ni2 0.25046	2 Ni2 0.24989
	2 Ni1 0.25206	2 Ni1 0.25171
	1 Si 0.27062	1 Si 0.27073
	(2 La 0.32905)	(2 Ce 0.32786)

susceptibility $\chi(T\rightarrow 0)\simeq 5.1\times 10^{-3}$ emu/mol followed by a smooth maximum and a Curie-Weiss-type high-temperature behavior which is analyzed in detail in Sec. IV B. Due to paramagnetic impurities, a small Curie-Weiss-type contribution, $\chi_{CW}(T)=C/(T-\Theta)$, occurs below about 10 K with $C\sim 10^{-3}$ emu K/mol in both samples.

The specific heat $C_p(T)$ of $CeNi_9Si_4$ and $LaNi_9Si_4$ is shown in Fig. 3 as C/T vs T. The low-temperature electronic and lattice contributions of a normal metal are given by $C_p=C_e+C_{ph}\simeq\gamma T+\beta T^3$ where γ is the Sommerfeld parameter and β is related to the low-temperature value of the Debye temperature, $\Theta_D^{LT}=(1944\times N/\beta)^{1/3}$ where $N=14$ is the number of atoms per formula unit. From the low-temperature fit of the $LaNi_9Si_4$ data (2–10 K, see the inset of Fig. 3 for a C/T vs T^2 presentation of these data) we obtain $\gamma=33(1)$ mJ/mol K^2 and $\beta=0.41(1)$ mJ/mol K^4 yielding $\Theta_D^{LT}=405(3)$ K. In the case of $CeNi_9Si_4$, where the specific heat includes contributions due to the presence of Ce-4f states, we observe an approximate temperature dependence $C_p(T)\simeq\gamma T+\beta T^3$ in the temperature interval 2–14 K, revealing a significant enhancement of the T-linear contribution $\gamma=155(5)$ mJ/mol K^2 compared to $LaNi_9Si_4$ with empty 4f states. This indicates the presence of heavy quasiparticles caused by Kondo interactions between conduction electrons and Ce-4f states. The Kondo contribution also increases the coefficient $\beta=0.58$ mJ/mol K^4 which is therefore not suited for an evaluation of the Debye temperature Θ_D^{LT} of $CeNi_9Si_4$.

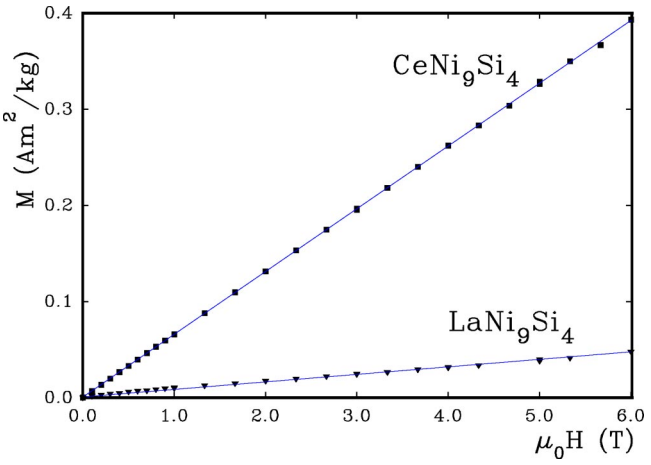

FIG. 1. The isothermal magnetization $M(H)$ of $CeNi_9Si_4$ and $LaNi_9Si_4$ measured at 2 K; the solid lines are linear.

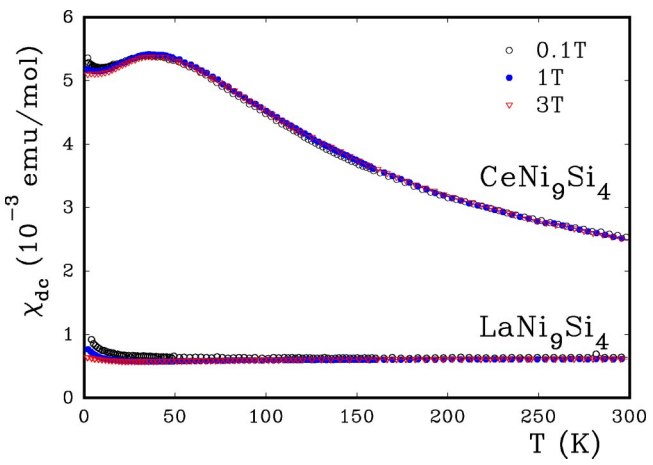

FIG. 2. The dc magnetic susceptibility of $\chi(T)$ of $CeNi_9Si_4$ and $LaNi_9Si_4$ measured at magnetic fields as labeled.

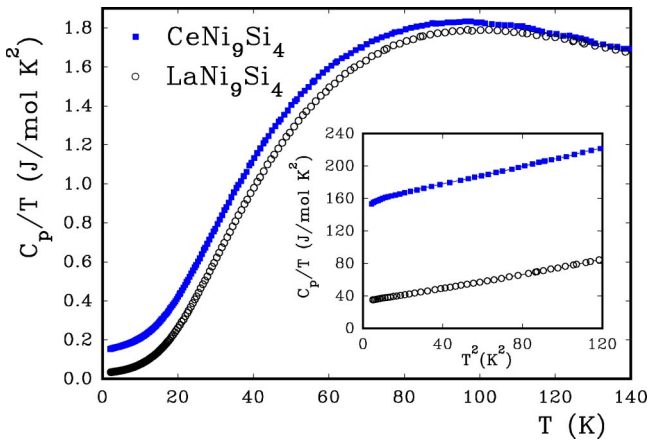

FIG. 3. The temperature-dependent specific heat $\Delta C_p(T)$ of $CeNi_9Si_4$ and $LaNi_9Si_4$ displayed as C/T vs T; the inset shows the low-temperature part as C/T vs T^2.

C. Transport measurements

The temperature-dependent electrical resistivities, $\rho(T)$, of $LaNi_9Si_4$ and $CeNi_9Si_4$ are depicted in Fig. 4. As expected from the magnetic-susceptibility and specific-heat data, Kondo interactions are present in $CeNi_9Si_4$. Accordingly, below about $T=20$ K $\rho(T)$ exhibits a regime of coherent Kondo scattering with $\rho(T)\simeq\rho_0+AT^2$ and an incoherent Kondo regime at elevated temperatures. A fit from 2 to 8 K yields for $CeNi_9Si_4$ the coefficient $A\simeq 0.020$ $\mu\Omega$ cm/K^2 and the residual resistivity $\rho_0\simeq 7.9$ $\mu\Omega$ cm. The latter is a measure for the number of lattice imperfections and defects and is found to be one order-of-magnitude lower for the stoichiometric RNi_9Si_4 samples (note, $\rho_0\simeq 7.7$ $\mu\Omega$ cm also for $LaNi_9Si_4$) than that of specimens prepared by the same procedure but with slightly off-stoichiometric Ni/Si composition (e.g., $CeNi_{8.8}Si_{4.2}$ with $\rho_0\sim 140$ $\mu\Omega$ cm, not shown). This further corroborates the existence of the stoichiometric 1-9-4 compound.

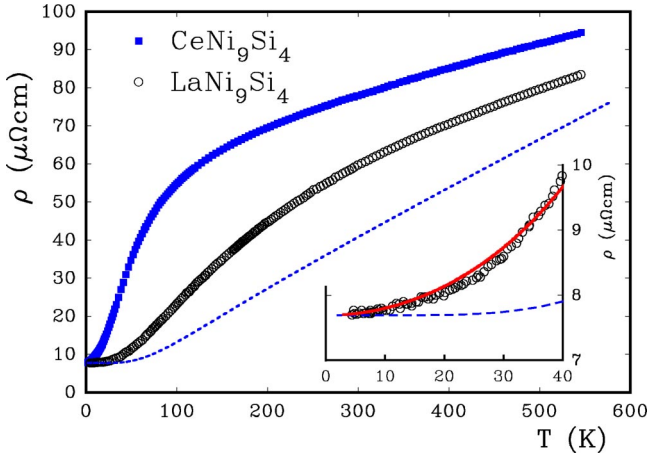

FIG. 4. The temperature-dependent electrical resistivity $\rho(T)$ of $CeNi_9Si_4$ and $LaNi_9Si_4$; the dashed line indicates the phonon contribution according to the Bloch-Grüneisen relation; the inset illustrates the analysis of the low-temperature resistivity of $LaNi_9Si_4$ (see text).

Since La and Ni ions do not carry local magnetic moments one expects the resistivity of $LaNi_9Si_4$ to be dominated by electron scattering by static defects and phonon excitations and, accordingly, to obey approximately the Bloch-Grüneisen (BG) relation

$$\rho_{\mathrm{BG}}(T)=\rho_0+\frac{4B}{\Theta_D}\left(\frac{T}{\Theta_D}\right)^5\int_0^{\Theta_D/T}\frac{z^5\mathrm{d}z}{(e^z-1)(1-e^{-z})}, \quad (1)$$

where B is a temperature-independent constant proportional to the electron-phonon interaction strength and Θ_D the Debye temperature. The latter should be of similar magnitude since $\Theta_D^{LT}=405$ K, obtained from the low-temperature specific-heat data. The resistivity $\rho(T)$ of $LaNi_9Si_4$ shown in Fig. 4, however, exhibits a pronounced curvature changing from positive to negative which is clearly incompatible with Eq. (1). This indicates that additional scattering mechanisms, e.g., due to electron-electron or paramagnon scattering, are of importance. The dashed line in Fig. 4 shows a temperature dependence according to the Bloch-Grüneisen model with parameters $\rho_0=8.3$ $\mu\Omega$ cm, $\Theta_D=405$ K, and $B=0.020$ $\mu\Omega$ cm K. Factor B has been chosen arbitrarily, but nevertheless, the condition that the result of Eq. (1) should not cross the experimental data defines an upper limit for the factor $B<0.022$ $\mu\Omega$ cm K. The arbitrary variation of B is hardly relevant below about 40 K where phonon scattering is small compared to the additional contribution revealed by the experimental data (see the inset of Fig. 4). Assuming electron-electron scattering with $\rho_{ee}(T)\simeq AT^2$ in the low-temperature limit allows an analysis according to $\rho(T)=\rho_{\mathrm{BG}}(T)+AT^2$ with the above parameters for ρ_0, B and Θ_D [$\rho_{\mathrm{BG}}(T)$ is indicated by the dashed line in Fig. 4]. The corresponding fit to $\rho(T)$ of $LaNi_9Si_4$ in the temperature interval 4–40 K (solid line, inset of Fig. 4) yields the coefficient $A\simeq 1.1\times 10^{-3}\mu\Omega$ cm/K^2. The mechanism behind the contribution $\rho_{ee}(T)$ is discussed in Sec. IV A.

The temperature-dependent thermoelectric power (TEP), $S(T)$, shown in Fig. 5, reveals for $CeNi_9Si_4$ rather large TEP values with $S_{\max}=+94$ μV/K at 33 K while the TEP of $LaNi_9Si_4$ ranges within the usual values of normal nonmagnetic metals [$|S(T)|<10$ μV/K]. Nevertheless, the temperature dependence of $S(T)$ of $LaNi_9Si_4$ shows a complex behavior with a tilde shape below about 400 K, but finally, above 600 K it approaches the usual high-temperature behavior of simple metals,[15] $S(T)=aT+b/T$ with $a=-9.1\times 10^{-3}$ μV/K^2 and $b=6.5\times 10^{+2}\mu$V which is indicated by the solid line in the inset of Fig. 5. $CeNi_9Si_4$ approaches the same high-temperature trend, $S(T)=aT+b/T$, yielding (above 600 K) the coefficients $a=-7.1\times 10^{-3}$ μV/K^2 and $b=2.8\times 10^{+3}$ μV, where the latter is significantly enhanced by spin disorder scattering. Note that in the high-temperature limit electron-defect and electron-spin disorder scattering rates are both constant, yielding contributions $S\propto 1/T$. The low-temperature behavior of $S(T)$ of $CeNi_9Si_4$ is discussed in Sec. IV B.

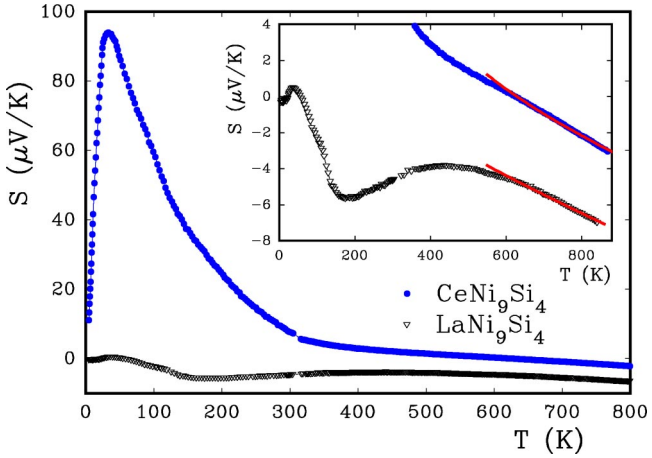

FIG. 5. The temperature-dependent thermopower $S(T)$ of $CeNi_9Si_4$ and $LaNi_9Si_4$; the inset gives a closer scale where the high-temperature fit according to the relation $S(T)=aT+b/T$ is indicated by solid lines.

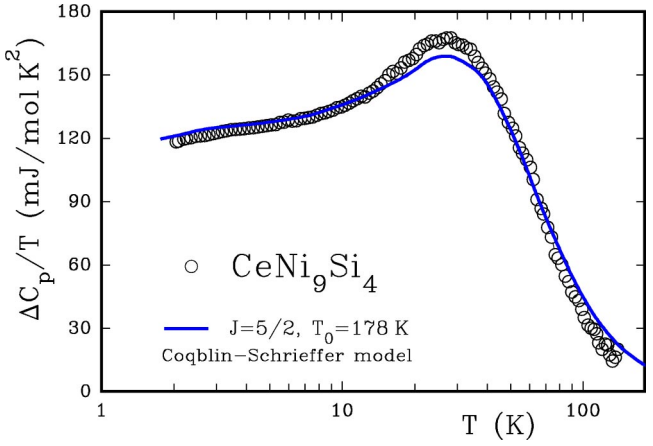

FIG. 6. The magnetic specific-heat contribution of $CeNi_9Si_4$ shown as $\Delta C_p(T)/T$ on a logarithmic temperature scale; the solid line corresponds to the Coqblin-Schrieffer model for a sixfold-degenerate ground-state with the characteristic temperature $T_0=178$ K.

IV. DISCUSSION

A. $LaNi_9Si_4$

The magnetic-susceptibility and specific-heat results presented in Sec. III B indicate for $LaNi_9Si_4$ a simple Pauli paramagnetic metallic behavior where the Ni-3d band is almost filled and La is in the nonmagnetic $4f^0$ state. We thus consider that a spin-fluctuation (paramagnon) mechanism or s-d-electron scattering is the reason for the appreciable curvature of the resistivity $\rho(T)$ and the low-temperature T^2 behavior discussed above. In order to rate the relevance of spin fluctuations in $LaNi_9Si_4$, the exchange enhancement of the Pauli susceptibility is analyzed. The temperature-independent susceptibility ($\chi_0 \simeq 0.6\times10^{-3}$ emu/mol, see above) contains contributions from the core diamagnetism, the Landau diamagnetism, and the Stoner-enhanced Pauli paramagnetism,

$$\chi_0=\chi_{core}+\chi_{\mathrm{Landau}}+\mathrm{S}\chi_{\mathrm{Pauli}}, \tag{2}$$

with $\chi_{\mathrm{Landau}}=-\mu_B^2N(E_f)/3(1+\lambda)^2$, $\chi_{\mathrm{Pauli}}=\mu_B^2N(E_f)$, and the Stoner factor $S=[1-IN(E_f)]^{-1}$ with I the exchange integral and $N(E_f)$ the electronic density of states at the Fermi level. Since the value of χ_{core} can simply be estimated using the data of Ref. 16 yielding -1.32×10^{-3} emu/mol for $LaNi_9Si_4$, the Stoner factor is evaluated from Eq. (2) via

$$S=\frac{\chi_0-\chi_{core}}{\mu_B^2N(E_f)}+\frac{1}{3(1+\lambda)^2}, \tag{3}$$

by using an estimate for the electron mass enhancement $\lambda=\lambda_{ep}+\lambda_{spin}$. Note that the electronic density of states $N(E_f)$ is determined from the electronic specific heat by $\gamma=(\pi^2/3)k_B^2(1+\lambda)N(E_f)$. For simple nonsuperconducting (or $T_c\leqslant1$ K) Pauli paramagnetic metals and intermetallic compounds the mass enhancement due to electron-phonon interactions λ_{ep} is typically 0.3–0.6 and the mass enhancement due to spin fluctuations $\lambda_{spin}\leqslant0.1$. Accordingly we assume $\lambda\sim0.4$–0.7 to be a reasonable range for the Pauli paramagnet $LaNi_9Si_4$. This yields with $\gamma=33$ mJ/mol K^2 a bare density of states $N(E_f)\sim9\pm2$ states/eV f.u. With the latter value for $N(E_f)$ one obtains with Eq. (3) a moderate Stoner-enhancement factor S ranging from 1.4 to 2 which hardly accounts for the considerable low-temperature contribution to the electrical resistivity as shown above, since the characteristic energy of the spin fluctuations, $k_BT_{sf}\simeq E_f/\mathrm{S}$, is of similar magnitude as the Fermi energy. Hence, we propose a Baber mechanism[17] (i.e., the scattering of s electrons by heavier d holes due to the screened Coulomb interaction in the case of the d-metal compound $LaNi_9Si_4$) as the dominating contribution, rather than a spin-fluctuation mechanism. This is corroborated by the experimental value obtained for the ratio $A/\gamma^2=1.0(1)\times10^{-6}$ $\mu\Omega$ cm(molK/mJ)^2 which matches the theoretical prediction by Rice[18] based on Baber's model for $A/\gamma^2\simeq0.9\times10^{-6}$ $\mu\Omega$ cm(mol K/mJ)^2. The latter calculation implies a band structure with a heavy d-band mass, i.e., $m_d\gg m_s$, which appears to be a realistic scenario for $LaNi_9Si_4$ but remains to be confirmed by band calculations.

B. $CeNi_9Si_4$

The magnetic-susceptibility, specific-heat, and transport data of $CeNi_9Si_4$ shown in Secs. III B and III C fit into a conventional Fermi-liquid picture with large $\chi(0)$ and γ values as compared to the nonmagnetic reference $LaNi_9Si_4$ and a low-temperature regime of coherent scattering indicating a nonmagnetic Kondo-lattice ground-state. The rather large spacing of the Ce sublattice (Ce-Ce distance ≈5.6 Å) suggests that intersite Ce-Ce interactions in $CeNi_9Si_4$ are very weak compared to other Kondo lattice systems (see Ref. 1 for a review) and gives good reason to analyze the specific heat and magnetic susceptibility of $CeNi_9Si_4$ in terms of the single-ion Coqblin-Schrieffer (CS) model.[19] Accordingly, we show in Fig. 6 a comparison of the magnetic contribution $\Delta C_p(T)$ to the specific heat of $CeNi_9Si_4$ (open circles; derived by subtracting the total specific heat of the nonmag-

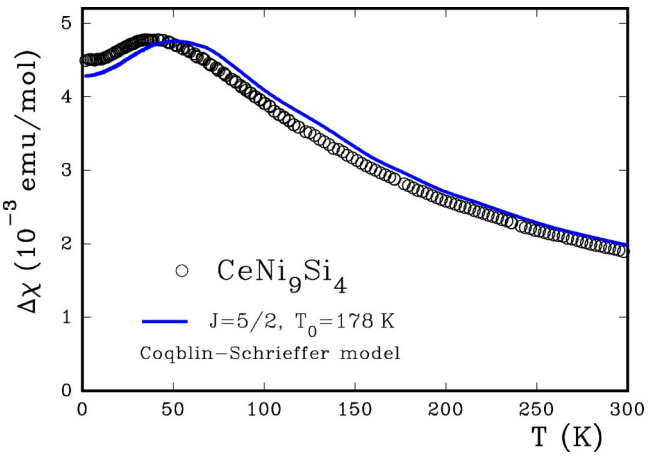

FIG. 7. The Kondo contribution to the magnetic susceptibility $\Delta\chi(T)=\chi_{dc}(T)-\chi_0$ of $CeNi_9Si_4$; the solid line corresponds to the Coqblin-Schrieffer model for a sixfold-degenerate ground-state with $T_0=178$ K.

netic reference $LaNi_9Si_4$) and the solution of the CS model obtained by Rajan[20] for a sixfold-degenerate ground-state ($J=5/2$) with a characteristic temperature $T_0=178$ K (solid line). The only free parameter of the CS model is the characteristic temperature T_0 which accounts for the energy scale of the Kondo interaction and is calculated from the relation $T_0=(N-1)\pi R/6\gamma^\star$, where $\gamma^\star=(\gamma-\gamma_0)\simeq 122$ mJ/mol K^2 is the $4f$ contribution to the Sommerfeld value ($\gamma_0=33$ mJ/mol K^2 is assumed to be equal to the $LaNi_9Si_4$ value). We note that due to the low fraction of Ce ions in $CeNi_9Si_4$ it is important to consider the actual Kondo ($4f$) contribution, while one usually approximates $\gamma^\star=(\gamma-\gamma_0)\simeq\gamma$ because $\gamma\gg\gamma_0$ is satisfied for the majority of heavy-fermion compounds.

The Kondo contribution to the Sommerfeld value $\gamma^\star$ and to the low-temperature susceptibility $\chi^\star(0)$ are linked to each other via the Fermi-liquid relation (see, e.g., Ref. 21), $g_J^2(J+1)\mu_B^2\gamma^\star=2\pi^2k_B^2\chi^\star(0)$, yielding for $\gamma^\star\simeq 122$ mJ/mol K^2 and $J=5/2$ the Kondo contribution to the magnetic susceptibility $\chi^\star(0)=4.32\times10^{-3}$ emu/mol which compares well with $[\chi(T\to0)-\chi_0]\simeq 4.5\times10^{-3}$ emu/mol. In other words, the experimentally obtained Wilson ratio,

$$R=\frac{\pi^2k_B^2\chi^\star(T\to0)}{g_J^2J(J+1)\mu_B^2\gamma^\star}\simeq 1.25, \tag{4}$$

is close to the value expected for an integer valent degenerate Ce^{3+} state,[22,23] $R=N/[N-1+(n_f-1)^2]=1.2$ for $N=6$ and $n_f=1$.

Having obtained the only free parameter of the degenerate CS model, $T_0=178$ K, from the analysis of the specific-heat data, there is a given solution for the magnitude and temperature dependence of the magnetic susceptibility $\chi^\star(T)$ without any further adjustable parameters. Accordingly, we compare the susceptibility $\Delta\chi=\chi(T)-\chi_0$ of $CeNi_9Si_4$ ($\chi_0=0.6\times10^{-3}$ emu/mol, the value obtained for $LaNi_9Si_4$) with $\chi^\star(T)$ predicted by the CS model[20] for sixfold-degenerate Ce^{3+} with the free-ion moment $\mu_{eff}=2.54\mu_B$ and $T_0=178$ K in Fig. 7. The reasonable quantitative agreement reveals two important points: first, it confirms the applicability of the integer valent Ce^{3+} limit assumed in the CS model and secondly, there is rather good agreement of the overall temperature dependence of the specific heat and magnetic susceptibility of $CeNi_9Si_4$ with the degenerate CS model which does not account for any crystalline electric field (CEF) effects. This indicates that the overall CEF splitting of the Ce^{3+} ground multiplet is smaller than the characteristic energy scale k_BT_0. A similar situation is observed for $YbCu_4Ag$ which is well accounted for by the fully degenerate CS model with $T_0\simeq 150$ K.[24,25] The relative magnitudes of CEF splitting and Kondo energy of the latter are indicated by the crossover of characteristic energy scales in the solid solution $YbCu_{5-x}Ag_x$ where for $x=1\to0$ a gradual reduction of the effective ground-state degeneracy accompanies the reduction of T_0, revealing an approximate overall CEF splitting $\Delta_{CEF}\sim 80$ K.[26] By analogy to the applicability of the degenerate CS model in the $YbCu_{5-x}Ag_x$ series we expect for $CeNi_9Si_4$ that $\Delta_{CEF}\sim 100$ K or smaller.

We already noted the large spacing of the Ce sublattice in $CeNi_9Si_4$ with a nearest-neighbor Ce-Ce distance of 5.6 Å, which appears to be the largest value among the commonly known cerium Kondo-lattice systems compiled in the review by Sereni.[1] $CeNi_9Si_4$ (not included in Ref. 1) is followed by $CeBe_{13}$ with a Ce-Ce distance of 5.2 Å which is, however, placed among the intermediate valent (IV) systems while the above analysis of the thermodynamic properties of $CeNi_9Si_4$ reveals an almost perfect agreement with the degenerate CS model presuming the integer valent limit $n_f=1$. Accordingly, $CeNi_9Si_4$ appears to be a prototype Kondo lattice with weak Ce-Ce intersite interaction and Ce ions remaining very close to the integer valent Ce^{3+} state. This is important in the context of the experimental and theoretical work on the diffusion thermopower of heavy-fermion compounds. The thermoelectric power $S(T)$ of Kondo-lattice systems frequently exhibits a sign change with a characteristic tilde shape ($\sim$) in the case of Yb compounds (an exception is $YbCu_4Ag$) and an inverted tilde shape in the case of Ce compounds. This, however, is not observed for the title compound $CeNi_9Si_4$ (see Fig. 5) and for few other exceptions e.g. $CeCu_6$ and IV systems such as $CePd_3$ and $CeBe_{13}$ (see Refs. 27–30).

A theoretical approach by Fischer[31] discusses the tilde shape of the diffusion thermopower $S_d(T)$ as a consequence of two competing contributions $S_d^1(T)$ and $S_d^2(T)$ that are of orders J^3V and J^2V in the coupling constant and, thus, of opposite sign when J, the s-f exchange integral, is negative. Thereby, $S_d^1(T)$ is the ''Kondo'' term and $S_d^2(T)$ is a ''resonance'' term which disappear for vanishing intersite actions. This view is corroborated by the above-mentioned exceptions $YbCu_4Ag$ and $CeCu_6$ where the sign change (tilde shape) is recovered, e.g., by Ag/Au or Cu/Au substitution, driving these systems towards a magnetic ground-state.[27,30] For the *clean limit* (i.e., without impurity scattering and intersite interactions), Fischer[31] obtained a simple solution for the low-temperature diffusion thermopower of the Anderson lattice yielding

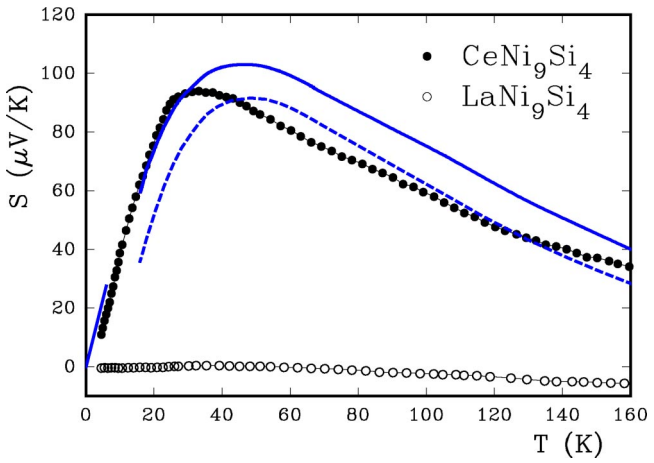

FIG. 8. The low-temperature thermoelectric power $S(T)$ of $CeNi_9Si_4$ (circles) in comparison with the result of Anderson lattice calculations by Cox and Grewe (the solid lines show clean-limit results and the dashed line indicates a correction according to the Kohler relation, see text for details).

$$S_d^{c.l.}(T) = 4.2\frac{k_B T}{|e| T_K} \tag{5}$$

with $k_B/|e| = 86\ \mu$V/K. The special case of negligible intersite spin interactions has also been analyzed by Cox and Grewe[32] considering a self-consistent approximation of the degenerate Anderson lattice in the Kondo limit. They obtained the same low-temperature clean limit [see Eq. (5)] and presented for the case of Ce^{3+} with $N=6$ and $T>0.2\ T_K$ a universal temperature dependence of $S(T/T_K)$ with a broad maximum $S_{max}=103\ \mu$V/K at $T/T_K \simeq 0.6$ (see Fig. 3 of Ref. 32). The Kondo temperature T_K can be obtained from $T_0 = 178$ K, invoking the Wilson number $W_J = T_K/T_0$. Various authors[33,34] have calculated the numerical value of W_J. A comparison, however, reveals some discrepancies for $J>1$. Schlottmann[34] reported $T_K/T_0 \simeq 0.43$ for $J=5/2$, yielding $T_K \sim 80$ K for the case of $CeNi_9Si_4$. The corresponding results according to the model by Cox and Grewe[32] [the low-temperature limit given by Eq. (5) and the numerical results for $T>0.2T_K$] are shown as solid lines in Fig. 8.

When comparing the TEP of $CeNi_9Si_4$ with the clean-limit calculations one has to consider that the approximation with negligible residual defect scattering and electron-phonon scattering compared to electron-electron scattering is, in particular, unrealistic at low temperatures where magnetic scattering vanishes as T^2, as well as at high temperatures where electron-phonon scattering gains weight. For a rough estimate of these limitations one can use the Kohler relation[35] for the total diffusion thermopower S_d due to different types of scattering mechanisms α, e.g. electron-defect ($S_{e,0}$), electron-electron (S_{ee}), and electron-phonon (S_{ep}) scattering, i.e.,

$$S_d = W^{-1} \sum_\alpha S_{d\alpha} W_\alpha, \tag{6}$$

with W being the electronic thermal resistance which approximately obeys the Matthiessen rule, $W = \Sigma_\alpha W_\alpha$, where W_α are the contributions due to particular scattering mechanisms α. W_α can be estimated considering the Wiedeman-Franz law, $W_\alpha(T) = \rho_\alpha(T)/L_\alpha T$, with $L_{imp} \approx L_{ep} \approx L_0 = 2.44 \times 10^{-8}$ W Ω/K^2 (L_0 is the Lorenz number). $L_{ee}(T)$ has been calculated for the Anderson lattice by Cox and Grewe.[32] For the temperature range in which S_{ee} is large compared to other contributions (see $LaNi_9Si_4$ as a reference), we further approximate $S_d(T) \approx S_{ee}(\rho_{ee}/\rho)$ with $\rho_{ee}(T) = \rho(T) - [\rho_0 + \rho_{ep}(T)]$ as indicated by the solid line in Fig. 8. $S_{ee}(T)$ is derived from the model of Cox and Grewe assuming $T_K \sim 80$ K. The corresponding result is indicated as a dashed line in Fig. 8, showing how the presence of electron-defect and electron-phonon scattering modifies the clean-limit Kondo contribution in the case of $CeNi_9Si_4$. This procedure improves the correspondence between the experimental and the theoretical results at elevated temperatures. At low temperatures, however, there is already a close agreement between the experimental data and the clean-limit result. This is unexpected, since $\rho_0 \gg \rho_{ee}$ at least below about 10 K; accordingly we expect $S(T) \propto T^2$ in the low-temperature limit. There is, of course, another important point which has to be taken into account: The analysis of the resistivity data of $LaNi_9Si_4$ indicates the presence of, at least, two types of conduction bands: *s*-type bands and *d* bands with a heavy band mass ($m_d \gg m_s$). A similar assumption is expected to hold for $CeNi_9Si_4$, i.e., the diffusion thermopower is composed not only of contributions due to different scattering mechanisms, but also of contributions of different bands $S_d(T) = \Sigma_j S_d^j \sigma^j/\sigma$ with σ^j being the electrical conductivity of band j.[15] This is particularly important at low temperatures where interband scattering is weak. Thus, Eq. (6) needs to be individually applied to each band contribution S_d^j. Notwithstanding these arbitrarily complex details, there is a rather good overall agreement with the absolute values predicted by the model calculations by Cox and Grewe, agreement which indeed corroborates the fact that the Ce-Ce intersite coupling is negligible with respect to the energy scale of Kondo interaction. We thus propose $T_0 > \Delta_{CEF} \gg T_{RKKY}$, where T_0, Δ_{CEF}, and T_{RKKY} are characteristic energy scales of the Kondo interaction, crystal-field splitting, and Ce-Ce intersite exchange interactions, respectively.

As evident from the above discussion, $CeNi_9Si_4$ fits to a Fermi-liquid picture, where $\chi(0)$ and γ obey the Wilson ratio. Accordingly, one expects a quantitative relation of $\chi(0)$ and γ also with respect to the A coefficient of the low-temperature resistivity $\rho(T) = \rho_0 + AT^2$. Compiling a large number of strongly correlated electron systems (mainly Ce and U compounds) Kadowaki and Woods[7] found empirically $A/\gamma^2 \sim 10^{-5}\ \mu\Omega$ cm(mol K/mJ)^2 while in the case of *d* metals Fermi-liquid theory[18] implies $A/\gamma^2 \simeq 0.9 \times 10^{-6}\ \mu\Omega$ cm(mol K/mJ)^2. The mean experimental trend for *d* elements (Os, Re, Pt, Pd, ...) reveals roughly $0.4 \times 10^{-6}\ \mu\Omega$ cm(mol K/mJ)^2. $CeNi_9Si_4$ yields $A/\gamma^2 = 0.83(8) \times 10^{-6}\ \mu\Omega$ cm(mol K/mJ)^2, which almost matches the reference $LaNi_9Si_4$ with $A/\gamma^2 \simeq 1.0(1) \times 10^{-6}\ \mu\Omega$ cm(mol K/mJ)^2. Both compounds are close to the *d*-metal calculation by Rice,[18] but appear to be one order-of-magnitude smaller than the Kadowaki-Woods ratio. Other

exceptions among Kondo-lattice systems with $A/\gamma^2 \leqslant 10^{-6}$ $\mu\Omega$ cm(mol K/mJ)^2 are $YbCu_4Ag$,[36] as well as the solid solution $YbCu_{5-x}Ag_x$ (Refs. 37 and 38) that exhibit a number of similarities to $CeNi_9Si_4$. Both systems are well described in terms of the CS model and do not show the typical tilde shape of the thermoelectric power (see above) which indicates $T_0 \gg T_{RKKY}$. The common feature $A/\gamma^2 \leqslant 10^{-6}$ $\mu\Omega$ cm(mol K/mJ)^2 of Ce and Yb systems with weak intersite coupling corroborates the frequently used argument that the larger Kadowaki-Woods ratio of heavy-fermion systems compared to *d* elements is due to RKKY interaction. There may be alternative explanations based on multiband features which can be relevant for both systems. If different conduction channels are considered, e.g., an *s* or *sp* band with weaker coupling and a *d* band with stronger coupling to the Kondo interaction, it is obvious that the coefficient *A* will not directly correspond to the mass-renormalized heavy quasiparticles, but to some weighted mean value of quasiparticle mass of the various conduction channels.

V. SUMMARY

A reinvestigation of the formation and crystal structure of the ternary $LaNi_9Si_4$ and $CeNi_{9-x}Si_{4+x}$ phases from single-crystal data revealed the existence of fully ordered stoichiometric $LaNi_9Si_4$ and $CeNi_9Si_4$ compounds isostructural to the $LaFe_9Si_4$ type (space group $I4/mcm$) with a rather narrow homogeneity region $x \leqslant 0.2$ for the formation of a single phase specimen annealed at 990°C.

The electronic ground-state properties of $LaNi_9Si_4$ and $CeNi_9Si_4$ were characterized by resistivity, thermopower, magnetic-susceptibility, and specific-heat measurements revealing for $LaNi_9Si_4$ metallic behavior with $\gamma = 33$ mJ/mol K^2 and moderately exchange enhanced Pauli paramagnetism with $\chi_0 \simeq 0.6 \times 10^{-3}$ emu/mol. The resistivity of $LaNi_9Si_4$ further reveals a contribution due to electron correlations $\rho_{ee}(T)$ that are attributed to Baber scattering of *s* electrons by heavier *d* holes, corroborated by the close agreement of the observed ratio $A/\gamma^2 \simeq 1.0 \times 10^{-6}$ $\mu\Omega$ cm(mol K/mJ)^2 with the theoretical one, $A/\gamma^2 \simeq 0.9 \times 10^{-6}$ $\mu\Omega$ cm(mol K/mJ)^2, calculated by Rice.[18]

$CeNi_9Si_4$ is a Kondo lattice with a large Sommerfeld value $\gamma = 155(5)$ mJ/mol K^2 and a nearly constant low-temperature susceptibility $\chi(T \to 0) \simeq 5.1 \times 10^{-3}$ emu/mol, yielding a Wilson ratio $R \simeq 1.25$ in close agreement with the value expected for an integer valent Ce^{3+} state. The temperature dependencies of the magnetic specific heat and susceptibility are well accounted for by the degenerate ($J = 5/2$) single-ion Coqblin-Schrieffer model with a characteristic temperature $T_0 \simeq 178$ K. The large spacing of the Ce sublattice in $CeNi_9Si_4$ with a minimum Ce-Ce distance of 5.6 Å suggests an exceptional position among cerium Kondo-lattices. The thermopower $S(T)$ of $CeNi_9Si_4$ is in close agreement with basic theoretical results calculated for the degenerate Anderson lattice in the Kondo limit without intersite interactions. The magnitude of the observed Kondo maximum $S_{max} = 94$ μV/K at 33 K matches well with the theoretical prediction $S_{max} \sim 100$ μV/K by Cox and Grewe.[32] $CeNi_9Si_4$, thus, appears to be a model-type Kondo-lattice with $T_0 > \Delta_{CEF} \gg T_{RKKY}$ where T_0, Δ_{CEF} and T_{RKKY} are characteristic energy scales of Kondo interaction, crystal-field splitting, and Ce-Ce intersite exchange coupling, respectively. A similar exceptional position among Yb-Kondo-lattice systems is considered for $YbCu_4Ag$ which in fact shows a number of analogies with $CeNi_9Si_4$, e.g., they have in common a rather small ratio $A/\gamma^2 \leqslant 10^{-6}$ $\mu\Omega$ cm(mol K/mJ)^2 which calls into question the universality of A/γ^2 assumed for all Kondo-lattice systems. According to the systematic tendency indicated by $CeNi_9Si_4$ and $YbCu_4Ag$, we suggest that a small ratio $A/\gamma^2 \leqslant 10^{-6}$ $\mu\Omega$ cm(mol K/mJ)^2 of a Kondo-lattice system can be an indication for either weak intersite exchange interactions and/or for different conduction channels with different coupling strengths to the Kondo interaction.

ACKNOWLEDGMENTS

This work was supported by the Austrian Science Foundation Fonds under Project Nos. P-13778 and P-15066-Phy and by the Kärntner Elektrititätsgesellschaft KELAG.

*Electronic address: michor@ifp.tuwien.ac.at

[1] J. Sereni, *Handbook on the Physics and Chemistry of Rare Earths*, edited by K.A. Gschneidner, Jr. and L. Eyring (North-Holland, Amsterdam, 1991), Vol. 15, pp. 1–59.

[2] H. von Löhneysen, J. Phys.: Condens. Matter **8**, 9689 (1996).

[3] F. Steglich, B. Buschinger, P. Gegenwart, M. Lohmann, R. Helfrich, C. Langhammer, P. Hellmann, L. Donnevert, S. Thomas, A. Link, C. Geibel, M. Lang, G. Sparn, and W. Assmus, J. Phys.: Condens. Matter **8**, 9909 (1996).

[4] O.I. Bodak, Kristallografiya **24**, 1280 (1979) [Sov. Phys. Crystallogr. **24**, 732 (1979)].

[5] O. Moze, C.H. de Groot, F.R. de Boer, and K.H.J. Buschow, J. Alloys Compd. **235**, 62 (1996).

[6] C. Rossel, K.N. Yang, M.B. Maple, Z. Fisk, E. Zirngiebl, and J.D. Thompson, Phys. Rev. B **35**, 1914 (1987).

[7] K. Kadowaki and S.B. Woods, Solid State Commun. **58**, 507 (1986).

[8] T. Roisnel and J. Rodriguez-Carvajal, Mater. Sci. Forum **378-381**, 118 (2001).

[9] Nonius Kappa CCD computer code Program Packages COLLECT, DENZO, SCALEPACK, SORTAV (Nonius, Delft, The Netherlands, 1998).

[10] G.M. Sheldrick, computer code SHELX-97, program for crystal structure refinement (University of Göttingen, Germany, 1997), Windows version by McArdle (National University, Galway, Ireland).

[11] E. Parthe, L. Gelato, B. Chabot, M. Penzo, K. Cenzual, and R. Gladyshevskii, *TYPIX, Standardized Data and Crystal Chemical Characterization of Inorganic Structure Types* (Springer-Verlag, Berlin, 1994).

[12] W.H. Tang, J.K. Liang, X.L. Chen, and G.H. Rao, J. Appl. Phys. **76**, 4095 (1994).

[13] M.F. Fedyna, V.K. Pecharskii, and O.I. Bodak, Inorg. Mater. (Transl. of Neorg. Mater.) **23**, 504 (1987).

[14] P. Rogl, *Handbook on the Physics and Chemistry of the Rare Earths*, edited by L. Eyring and K.A. Gschneidner, Jr. (North-Holland, Amsterdam, 1985), Vol. 7, pp. 1–264.
[15] F.J. Blatt, P.A. Schroeder, C.L. Foiles, and D. Greig, *Thermoelectric Power of Metals* (Plenum, New York, 1976).
[16] P.W. Selwood, *Magnetochemistry* (Interscience, New York, 1956), p. 78.
[17] W.G. Baber, Proc. R. Soc. London, Ser. A **158**, 133 (1937).
[18] M.J. Rice, Phys. Rev. Lett. **20**, 1439 (1968).
[19] B. Coqblin and R.J. Schrieffer, Phys. Rev. **185**, 847 (1969).
[20] V.T. Rajan, Phys. Rev. Lett. **51**, 308 (1983).
[21] P. Schlottmann, *Theory of Heavy Fermions and Valence Fluctuations* (Springer, Berlin, 1985), p. 68.
[22] N. Read and D.M. News, J. Phys. C **16**, L1055 (1983).
[23] A.C. Hewson and J.W. Rasul, J. Magn. Magn. Mater. **47-48**, 339 (1985).
[24] M.J. Besnus, P. Haen, N. Hamdaoui, A. Herr, and A. Meyer, Physica B **163**, 571 (1990).
[25] P. Schlottmann, J. Appl. Phys. **73**, 5412 (1993).
[26] H. Michor, K. Kreiner, N. Tsujii, K. Yoshimura, K. Kosuge, and G. Hilscher, Physica B **319**, 277 (2002).
[27] R. Casanova, D. Jaccard, C. Marcenat, N. Hamdaoui, and M.J. Besnus, J. Magn. Magn. Mater. **90-91**, 587 (1990).
[28] U. Gottwick, R. Held, G. Sparn, F. Steglich, K. Vey, W. Assmus, H. Rietschel, G.R. Stewart, and A.L. Giorgi, J. Magn. Magn. Mater. **63-64**, 341 (1987).
[29] B.D. Rainford, A.T. Adroja, and J.M.E. Geers, Physica B **199-200**, 556 (1994).
[30] E. Bauer, Adv. Phys. **40**, 417 (1991).
[31] K.H. Fischer, Z. Phys. C **76**, 315 (1989).
[32] D.L. Cox and N. Grewe, Z. Phys. C **71**, 321 (1988).
[33] A.C. Hewson and J.W. Rasul, J. Phys. C **16**, 6799 (1983).
[34] P. Schlottmann, Z. Phys. C **51**, 223 (1983).
[35] M. Kohler, Z. Phys. **126**, 481 (1949).
[36] T. Graf, J.M. Lawrence, M.F. Hundley, J.D. Thompson, A. Lacerda, E. Haanappel, M.S. Torikachvili, Z. Fisk, and P.C. Canfield, Phys. Rev. B **51**, 15 053 (1995).
[37] N. Tsujii, J. He, F. Amita, K. Yoshimura, K. Kosuge, H. Michor, G. Hilscher, and T. Goto, Phys. Rev. B **56**, 8103 (1997).
[38] N. Tsujii, J. He, K. Yoshimura, K. Kosuge, H. Michor, K. Kreiner, and G. Hilscher, Phys. Rev. B **55**, 1032 (1997).